

University of Groningen

## Intrinsic self-healing thermoset through covalent and hydrogen bonding interactions

Araya-Hermosilla, R.; Lima, G. M. R.; Raffa, P.; Fortunato, G.; Pucci, A.; Flores, Mario E.; Moreno-Villoslada, I.; Broekhuis, A. A.; Picchioni, F.

*Published in:*  
European Polymer Journal

*DOI:*  
[10.1016/j.eurpolymj.2016.06.004](https://doi.org/10.1016/j.eurpolymj.2016.06.004)

**IMPORTANT NOTE:** You are advised to consult the publisher's version (publisher's PDF) if you wish to cite from it. Please check the document version below.

*Document Version*  
Publisher's PDF, also known as Version of record

*Publication date:*  
2016

[Link to publication in University of Groningen/UMCG research database](#)

### *Citation for published version (APA):*

Araya-Hermosilla, R., Lima, G. M. R., Raffa, P., Fortunato, G., Pucci, A., Flores, M. E., Moreno-Villoslada, I., Broekhuis, A. A., & Picchioni, F. (2016). Intrinsic self-healing thermoset through covalent and hydrogen bonding interactions. *European Polymer Journal*, *81*, 186-197.  
<https://doi.org/10.1016/j.eurpolymj.2016.06.004>

### **Copyright**

Other than for strictly personal use, it is not permitted to download or to forward/distribute the text or part of it without the consent of the author(s) and/or copyright holder(s), unless the work is under an open content license (like Creative Commons).

The publication may also be distributed here under the terms of Article 25fa of the Dutch Copyright Act, indicated by the "Taverne" license. More information can be found on the University of Groningen website: <https://www.rug.nl/library/open-access/self-archiving-pure/taverne-amendment>.

### **Take-down policy**

If you believe that this document breaches copyright please contact us providing details, and we will remove access to the work immediately and investigate your claim.

*Downloaded from the University of Groningen/UMCG research database (Pure): <http://www.rug.nl/research/portal>. For technical reasons the number of authors shown on this cover page is limited to 10 maximum.*



# Intrinsic self-healing thermoset through covalent and hydrogen bonding interactions

R. Araya-Hermosilla<sup>a</sup>, G.M.R. Lima<sup>a</sup>, P. Raffa<sup>a</sup>, G. Fortunato<sup>a</sup>, A. Pucci<sup>b</sup>, Mario E. Flores<sup>c</sup>, I. Moreno-Villoslada<sup>c</sup>, A.A. Broekhuis<sup>a</sup>, F. Picchioni<sup>a,\*</sup>

<sup>a</sup> Department of Chemical Engineering/Product Technology, University of Groningen, Nijenborgh 4, 9747AG Groningen, The Netherlands

<sup>b</sup> Department of Chemistry and Industrial Chemistry, University of Pisa, Via Moruzzi 13, 56124 Pisa, Italy

<sup>c</sup> Instituto de Ciencias Químicas, Facultad de Ciencias, Universidad Austral de Chile, Casilla 567, Valdivia, Chile

## ARTICLE INFO

### Article history:

Received 8 April 2016

Received in revised form 2 June 2016

Accepted 4 June 2016

Available online 4 June 2016

### Keywords:

Paal-Knorr chemical modification

Diels-Alder reaction

Hydrogen bonding interactions

Tuneable self-healing thermoset

Recycling

## ABSTRACT

The intrinsic self-healing ability of polyketone (PK) chemically modified into furan and/or OH groups containing derivatives is presented. Polymers bearing different ratios of both functional groups were cross-linked via furan/bis-maleimide (Diels-Alder adducts) and hydrogen bonding interactions (aliphatic and aromatic OH groups). The resulting thermosets display tuneable softening points (peak of  $\tan(\delta)$ ) from 90 to 137 °C as established by DMTA. It is found that the cross-linked system containing only furan groups shows the highest softening temperature. On the other hand, systems displaying the combination of Diels-Alder adducts and hydrogen bonding (up to 60 mol % of –OH groups) do not show any change in modulus between heating cycles (*i.e.* factually a quantitative recovery of the mechanical behaviour). It is believed that the novelty of these tuneable thermosets can offer significant advantages over conventional reversible covalent systems. The synergistic reinforcement of both interactions resists multiple heating/healing cycles without any loss of mechanical properties even for thermally healed broken samples.

© 2016 Elsevier Ltd. All rights reserved.

## 1. Introduction

Over the last few decades, researchers working on the design and optimization of plastic materials have reported considerable improvements (*e.g.* in mechanical properties of recycled materials) often stimulated by societal driven demands in terms of sustainability, enhancement of material quality and value-add services [1,2]. However, despite all the efforts, it is widely recognized that plastic recycling is still facing relevant problems regarding collection, separation, cleaning, processing chemistry and flow markets for recycled products [3–6].

As an attempt for improvements in this matter, the European Commission has categorized the waste treatment according to the most environmentally favourable strategies. The “waste hierarchy” establishes as priority the *prevention* followed by the *reuse* and *recycling* of waste, while the less favourable strategies are the *recovery* and *disposal* [7]. In the particular case of plastics, suitable materials for recycling are subjected to the availability of treatment technology and markets [8,9]. For instance, the most used procedures for thermoplastics recycling are the physical and chemical approaches. The physical recycling is realized by the grinding and re-melting of thermoplastics to produce a material with equal, similar or completely

\* Corresponding author.

E-mail address: [f.picchioni@rug.nl](mailto:f.picchioni@rug.nl) (F. Picchioni).

different properties compared to the original one. On the other hand, the chemical recycling turns thermoplastics into monomers or oligomers (by the addition of chemical additives and processing conditions) to be used as raw materials for the production of new polymers [10].

Thermosets unlike thermoplastics, cannot be recycled by using the above mentioned approaches (e.g. re-melted/re-shaped or chemical reduction to monomers) since they degrade or decompose. In this context, (thermally) reversible thermoset materials represent an accessible solution due to their remarkable ability of being mended and recycled (according to a “cradle to cradle” approach) in order to prolong their use after their first service life [11]. Several scientific articles have reported the ability of thermoset polymers to be repaired in different ways. These include the incorporation of low molecular weight additives in the form of capsules as healing agent after damage events (extrinsic self-repair) [12–16], but also the functionalization of raw non-reworkable polymers that can heal cracks as a consequence of an external stimuli like heat [17–20] and light [21–25] (intrinsic self-repair). The last approach relies on the chemical modification of the base polymer with functional groups able to undergo a reversible reaction as function of the presence/absence of the external stimulus. Diels-Alder or hydrogen bonding active groups are indeed often employed to prepare polymer networks with thermally reversible properties [26,27]. Therefore, in a fracture event, the healing process can be performed by the combination of covalent (Diels-Alder) and or non-covalent (H-bonds) reversible interactions. It is ideal as the intrinsic self-healing ability (i.e. bonds reconnection) of both functional groups plays a crucial role in supporting the recovery of the network (e.g. dimensional stability) at different levels of energy (i.e. complementary reinforcement of chemical and physical interactions). Therefore, the healing process can be achieved under different conditions (e.g. temperature) just by controlling the ratio between the introduced functional groups. These advantages have recently triggered the research on thermoset systems with tuneable chemical reversibility and mechanical properties (e.g. polymers containing reversible [20,26,28] and non-reversible [29–31] covalent interactions in combination with hydrogen bonding). However, the design of this kind of materials still faces problems in terms of lengthy, costly and cumbersome synthetic steps, thus hindering any application at industrial scale.

Against this drawback, we recently reported on the novel thermally self-healing properties of polymer networks containing reversible covalent and non-covalent interactions based on aliphatic polyketones [20,32]. In order to prepare the target materials, we started modifying alternating aliphatic polyketone (PK) into new polymers by using the Paal-Knorr reaction, i.e. the chemical modification of the di-carbonyl arrangement of PK into pyrrole groups bearing furan or amine active groups [20]. This synthetic pathway offers several advantages like high yield under relatively mild condition (100 °C) and fast reaction kinetics (4 h) even without any catalyst, with water as the only by-product. Subsequently, the modified PK was covalently cross-linked through the Diels-Alder (DA) reaction by using bis-maleimide. The simultaneous presence in the modified polymers of both interactions (H-bonding and DA adducts) resulted in networks with softening points from 100 to 185 °C. Remarkably, the materials retained quantitative modulus values after multi heating-healing cycles. However, they also displayed an increase in the softening point between cycles, which was ascribed to the formation of irreversible cross-linking points via the reaction of the pendant amine groups with the unreacted carbonyls along the backbone [20]. In order to overcome this drawback, this work is focused on preparing tuneable reversible thermosets through the synergistic cooperation of covalent and non-covalent interactions. These materials should then be able to display reversible properties after several heating/healing and recycling cycles. In principle, this can be achieved by using OH functional groups (instead of amino ones) as hydrogen bonding active moieties, thus avoiding any side reaction with the unreacted carbonyls along the backbone. In order to establish more clearly the role of the OH-groups, reference polymers displaying the same pyrrolic backbone of the target ones were functionalized with less reactive moieties without OH groups.

After modification, the polymers are covalently cross-linked via furan/maleimide Diels-Alder adducts and hydrogen bondings. The thermal and mechanical behaviour is then studied by differential scanning calorimetry DSC and dynamic mechanical thermal analysis (DMTA) to determine the reversibility, rework-ability and intrinsic self-healing ability of the thermoset polymers.

## 2. Experimental section

### 2.1. Reagents

The alternating aliphatic polyketone, terpolymer of carbon monoxide with 30% of ethylene and 70% of propylene per mol (PK30, Mw 2687 g/mol), on the basis of the total olefin content, was synthesized according to a reported procedure [33,34]. The resulting product presents a 43% of carbonyl content on the basis of the total molecular weight of polymer. Furfurylamine (**Fu**) was freshly distilled (Aldrich,  $\geq 99\%$ ). 3-Amino-1-propanol (**Ap**) (Acros, The Netherlands), 2-(4-hydroxyphenyl) ethylamine (tyramine **Ty**) (Sigma Aldrich 99%), 2,5-hexanedione (Sigma Aldrich 98%), butylamine (**Ba**) (Sigma Aldrich 99%) benzylamine (**Bea**) (Sigma Aldrich 99%), 1-Propanol, Milli-Q water, (1,1-(methylenedi-4,1-phenylene) bis-maleimide (**b-Ma**) (Sigma Aldrich 95%), chloroform (CHCl<sub>3</sub> Laboratory-Scan, 99.5%), were purchased and used as received. Deuterated dimethylsulfoxide (DMSO-*d*<sub>6</sub>, Sigma Aldrich,  $\geq 99.9$  atom%) was used as solvent for <sup>1</sup>H NMR measurements.

### 2.2. Model component reaction

Model reactions between stoichiometric amounts of 2,5-hexanedione (8.7 mmol) with either furfurylamine (previously reported by our group [35]), 3-amino-1-propanol (0.65 g) or tyramine (1.2 g) were carried out in order to identify the

presence of any side product. The reactants were poured into a flask provided with a reflux condenser and transferred to the microwave apparatus. The reactions were performed at 100 °C (200 W) for two hours in bulk in the case of 2,5-hexanedione with 3-amino-1-propanol and using 1-propanol as solvent (10 wt%) in the case of 2,5-hexanedione with tyramine. Thereafter, the organic solvent was removed in a vacuum oven at 50 °C for 24 h and the by product (H<sub>2</sub>O) was removed in a freeze dryer for 72 h.

### 2.3. Polyketone modification

The chemical modification of PK30 was performed by two different methods (**1** conventional oil bath and **2** microwave oven). In both methods, the reaction conditions were set at different molar ratios between 1,4-dicarbonyl of PK30 and amine compounds. PK30-**Fu** and PK30-**Fu-Ap** were prepared in a conventional oil bath as well as the reference polymers PK30-**Ba** and PK30-**Bea**, while PK-**Fu** and PK-**Fu-Ty** by using the microwave oven.

In the case of **1**, the reactions were carried out in bulk in a sealed 250 mL round-bottomed glass reactor with a reflux condenser, a U-type anchor impeller, and an oil bath for heating. After 60 g of PK30 were preheated to a liquid state at 100 °C, the amine compounds furfurylamine and/or 3-amino-1-propanol (butylamine or benzylamine for reference polymers) were added dropwise to the reactor during the first 20 min (mmol equivalent to 20–80% aimed conversion). The stirring speed was set at a constant value of 600 rpm and the reaction time was set at 4 h.

Procedure number **2** is employed in order to reduce the reaction time for the chemical modification of PK30 into polymers bearing Fu and aromatic-OH groups [36]. In a typical experiment, a mixture of polymer (4.0 g PK30) with furfurylamine and/or tyramine (mmol equivalent to 35–80% aimed conversion) was pre-dissolved in 1-propanol (≈10 wt% of polymer) and then poured into a flask provided with a reflux and transferred to the microwave apparatus. The microwave power was set at 200 W to keep a constant temperature of 100 °C for 2 h. After reaction, the solvent was removed using rotary evaporation. Finally, the products were dried under vacuum at 50 °C for 24 h.

In both procedures, the resulting polymers were frozen with liquid nitrogen, crushed to powdery samples and washed three times with deionized Milli-Q water to remove unreacted amine compounds, if any. After filtering and freeze drying, light-brown polymers were obtained as final products. The carbonyl conversion ( $C_{co}$ ) of PK30 can be calculated by:

$$C_{co} = \frac{y}{y+x} \cdot 100 \quad (1)$$

where  $x$  and  $y$  represent the moles of di-ketone and pyrrolic units after conversion, respectively.  $y$  can be calculated as follows:

$$y = \frac{N}{A_{m(N)}} \quad (2)$$

where  $N$  represents the grams of nitrogen in the product according to elemental analysis and  $A_{m(N)}$  represents the atomic mass of nitrogen.  $x$  can be calculated as follows:

$$g_p = x \cdot M_w^{pk} + y \cdot M_w^y \quad (3)$$

where  $g_p$  represents the grams of the final product after conversion,  $M_w^y$  the molecular weight of the pyrrolic unit (*i.e.* pyrrolic units bearing either Fu, OH or both functional groups) and  $M_w^{pk}$  the molecular weight of the 1,4 di-ketone unit. Then we can conclude that:

$$x = \frac{g_p - y \cdot M_w^y}{M_w^{pk}} \quad (4)$$

The conversion efficiency  $\eta$  can be defined as the ratio between the final carbonyl conversion  $C_{co}$  and the targeted one according to the amount of polymer and amine compounds provided in the feed ( $C_{co}^{feed}$ ):

$$\eta = \frac{C_{co}}{C_{co}^{feed}} \times 100 \quad (5)$$

The  $C_{co}^{feed}$  is calculated as follow:

$$C_{co}^{feed} = \frac{Mol_{amine}}{Mol_{PK30}} \cdot 100 \quad (6)$$

with  $Mol_{amine}$  representing the moles of amine compounds and  $Mol_{PK30}$  the moles of di-carbonyl units in the feed.

### 2.4. Diels-Alder reaction

The DA reaction of PK30-Fu and PK30-Fu-OH (2.0 g) with bis-maleimide was carried out in a ratio 1:1 between the furan moiety and the maleimide group using chloroform as solvent (≈10 wt% of polymer) in a 100 mL round-bottomed flask

equipped with a magnetic stirrer and a reflux condenser. The reaction mixture was heated up to 50 °C for 24 h to form the DA adducts. After reaction, the cross-linked polymers were dried at 50 °C under vacuum overnight to remove the solvent.

### 2.5. Characterization

The elemental analysis was performed using an Euro EA elemental analyzer.  $^1\text{H}$  NMR spectra were recorded on a Varian Mercury Plus 400 MHz apparatus using  $\text{DMSO-}d_6$  as solvent (residual resonance at 2.5 ppm). FT-IR spectra were recorded using a Perkin-Elmer Spectrum 2000. The samples (pellets) were prepared by mixing potassium bromide (KBr) with the polymers at (1.5 wt%). The pills were then kept in an oven for 24 h at 50 °C to remove residual water. DSC analysis was performed on a TA-Instrument DSC 2920 under  $\text{N}_2$  atmosphere. The samples for DSC were weighed (10–17 mg) in an aluminium pan, which was then sealed. The samples were first heated from 0 to 180 °C and then cooled to 0 °C. Four cycles were performed at 10 °C/min scanning rates. GPC measurements were performed with a HP1100 Hewlett-Packard to evaluate possible side reactions of the polymers during the modification step, if any. The equipment consists of three  $300 \times 7.5$  mm PLgel 3  $\mu\text{m}$  MIXED-E columns in series and a GBC LC 1240 IR detector. The samples were dissolved in THF at a concentration of 1 mg/mL. THF was used as eluent at a flow rate of 1 mL/min at a temperature of 40 °C. The calibration curve was realized using Polystyrene as standard and the data were determined using PSS WinGPC software. The samples for DMTA analysis were prepared by compression molding of 500 mg of cross-linked PK30-Fu/Bis-maleimide and PK30-Fu-OH/Bis-maleimide into rectangular bars of 6 mm in width, 1 mm in thickness, and 54 mm in length at 150 °C for 30 min under a pressure of 40 bar. The samples were then kept in an oven at 50 °C for 24 h aimed at thermal healing treatment. The DMTA analysis of the bars was conducted on a Rheometrics scientific solid analyzer (RSA II) under an air environment using the dual cantilever mode at an oscillation frequency of 1 Hz and a heating rate of 3 °C/min.

## 3. Results and discussion

### 3.1. Model component Paal-Knorr reaction

Model reactions of 2,5-hexanedione (*i.e.* representative for the di-carbonyl moieties along PK30 backbone) with aliphatic and aromatic amines were performed. The present Paal-Knorr reaction resulted in the formation of a pyrrole group, ultimately yielding pyrrole-furane [35] and pyrrole-OH derivatives (see Fig. 1 for NMR spectra). In Fig. 1A it is possible to notice the signal of protons associated to the pyrrole ring at 5.6 ppm, the presence of  $\text{CH}_2$  units at 1.6, 3.4 and 3.8 ppm and the proton signal at 4.6 corresponding to the OH group. In a similar way, Fig. 1B displays the proton signals associated to the pyrrole ring at 5.6 ppm, the presence of  $\text{CH}_2$  units at 2.7 and 3.8 ppm, the proton signals associated to the aromatic ring at 6.6 and 6.9 ppm and the proton signal corresponding to the OH group at 9.2. In both cases, no relevant by-products are observed and, in particular, no evidence is found for a possible reaction between the  $-\text{OH}$  and carbonyl groups.

### 3.2. Paal-Knorr reaction of PK30

The aim of this work is the preparation of thermo-reversible polymer networks by combining reversible covalent bonding (DA and r-DA sequence) using PK-furan derivatives together with OH groups. We started with the conversion of PK into the PK-Furan-OH (*i.e.* aliphatic or aromatic OH derivatives) by Paal-Knorr reaction by using a mixture of the corresponding amino compounds (Fig. 2).

Since the amine conversion is practically quantitative in this reaction [20,35], this easily allows (in principle) the preparation of materials characterized by different conversion values of carbonyl groups. The reactions between PK30 and aliphatic/aromatic amine compounds were carried out according to different molar ratios as expressed in the sample nomenclature (Table 1). The corresponding samples are coded as PK30-Fu $_{x_1}$ -OH $_{x_2}$  with  $x_i$  being the mol percentage of amine with respect to carbonyl groups in the feed while OH represents a common symbol for 3-amine-1-propanol (Ap) or tyramine (Ty).

The obtained results (Table 1) include the carbonyl conversion ( $C_{\text{CO}}$ , as measured experimentally) and the relative efficiency for the main conversion ( $\eta$ ). Indeed, in terms of conversion efficiency, almost all used amines display values around 100%, thus testifying the easiness of the reaction as well as its quantitative yield [20,35]. Moreover, the reported data in Table 1 confirm that the use of microwaves can significantly shorten the reaction time with no detrimental effect on the conversion values [20,35,37,38]. However, minor detrimental effects were observed on the molecular weight of polymers modified with only tyramine according to GPC data (SI1). Besides, slightly lower  $\eta$  values are obtained for PK30-Fu-Ty when the concentration of Fu is increased in agreement with the sensitivity of this reaction to steric hindrance [38,39]. The  $^1\text{H}$  NMR spectra of the polymers bearing different ratios of pendant groups are displayed in Fig. 3. As mentioned earlier, model compounds can be used as simple representations of complex polymeric systems. In the case of Fig. 3, the overlapping and broad character of many peaks was easily overcome using the information obtained from the model compounds. Fig. 3a shows signals that belong to protons associated to pyrrole rings at 5.6 ppm, the presence of  $\text{CH}_2$  units attached to the pyrrol groups in the OH moiety at 3.3 and 3.7 ppm and the proton signal of OH groups at 4.6 ppm. In a similar way, the presence of  $\text{CH}_2$  unit between the pyrrol and furan group is noticed at 4.9 ppm and proton signals of furan moieties at 6.1, 6.3 and 7.5 ppm are observed. Fig. 3b evidences the formation of the pyrrole ring at 5.6 ppm, the presence of  $\text{CH}_2$  unit attached to the pyrrol group in the OH moiety at 3.8 ppm, the protons associated to the benzene ring at 6.6 and 6.9 ppm, and the protons of OH groups at 9.2 ppm.

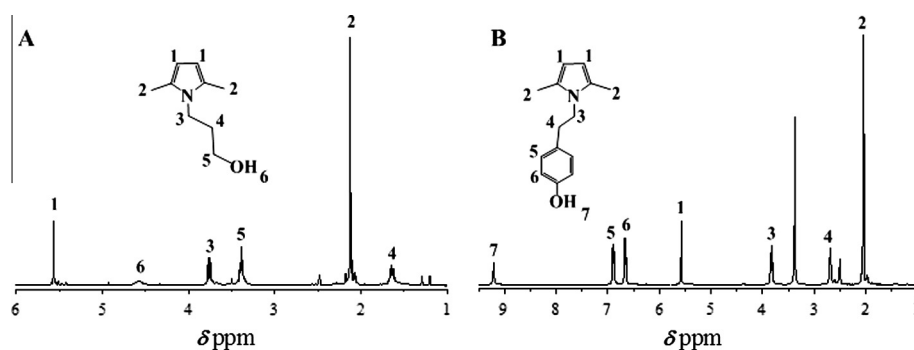


**Fig. 1.**  $^1\text{H}$  NMR spectra of model compound reaction between 2,5-hexanedione and 3-amino-1-propanol (A) and tyramine (B). The peak at 3.3 ppm can be assigned to residual water.

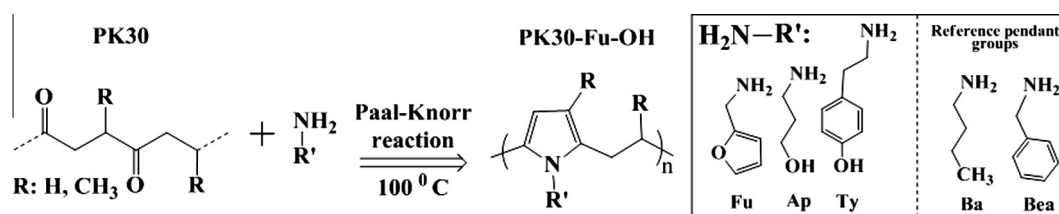


**Fig. 2.** Schematic representation of polyketone PK functionalized with aliphatic and aromatic amines by Paal-Knorr reaction.

**Table 1**

Experimental conditions and results of the chemical modification of PK30 using different ratios between aliphatic and aromatic amine compounds ( $X_{\text{NH}_2}$ ).

Oil bath	$X_{\text{NH}_2/\text{C}=\text{O}}$	$X_{\text{NH}_2}$ (moles)	$\text{C}_{\text{CO}}^{\text{a}}$ (%)	$\eta^{\text{b}}$ (%)	Microwave	$X_{\text{NH}_2/\text{C}=\text{O}}$	$X_{\text{NH}_2}$ (moles)	$\text{C}_{\text{CO}}^{\text{a}}$ (%)	$\eta^{\text{b}}$ (%)
PK30-Ba80 <sup>c</sup>	0.8	0.365	78	98	PK30-Bea80 <sup>c</sup>	0.8	0.024	69	86
PK30-Fu20	0.2	0.091	19	99	PK30-Fu80	0.8	0.024	68	85
PK30-Fu40	0.4	0.182	39	99	PK30-Ty35	0.35	0.011	34	97
PK30-Fu60	0.6	0.274	58	98	PK30-Ty50	0.5	0.015	49	98
PK30-Fu80	0.8	0.365	76	96	PK30-Ty65	0.65	0.020	63	97
PK30-Ap20	0.2	0.091	15	75	PK30-Ty80	0.8	0.024	76	95
PK30-Ap40	0.4	0.182	36	90	PK30-Fu65-Ty15	0.8	0.024	60	75
PK30-Ap60	0.6	0.274	57	95	PK30-Fu50-Ty30	0.8	0.024	67	83
PK30-Ap80	0.8	0.365	79	99	PK30-Fu35-Ty45	0.8	0.024	73	91
PK30-Fu20-Ap60	0.8	0.365	77	96	PK30-Fu15-Ty65	0.8	0.024	73	91
PK30-Fu40-Ap40	0.8	0.365	78	97					
PK30-Fu60-Ap20	0.8	0.365	78	98					

<sup>a</sup> % conversion of carbonyl groups.

<sup>b</sup>  $\eta$  conversion efficiency.

<sup>c</sup> Reference samples: PK30-Ba (butylamine) and PK30-Bea (benzylamine) same polymer structure but not bearing active functional Fu (furan) or OH (propanol, phenol) groups.

The area below each signal changes according to the number of protons that belong to each functional group whereas the intensity of the signal assigned to the pyrrole ring remains constant. This trend well agrees with the formation of the desired structure, although a quantitative estimation is affected by peak overlapping. Furthermore, spectral data obtained by FT-IR analysis corroborate the  $^1\text{H}$  NMR results. Fig. 4A displays FT-IR spectra for PK30-Fu-Ap at two different conversion values. We start by noticing the appearance of broad peaks around  $3400\text{ cm}^{-1}$  that belong to the OH group experiencing intermolecular hydrogen bonding, the pyrrole ring at  $3115$  and  $1505\text{ cm}^{-1}$  and the furan moiety at  $3150$ ,  $1145$  and  $738\text{ cm}^{-1}$ .

The same holds true for PK30-Fu-Ty (Fig. 4B) with the expected appearance of absorptions related to the benzyl ring at  $1613$  and  $828\text{ cm}^{-1}$ . In both cases (Fig. 4A and B) the intensity between the peaks of furan and OH groups change as a function of conversion. Fig. 4C displays the magnification of the PK30-Fu-Ty spectra in the C–H bending region for polymers bearing only furan or both furan and benzyl-OH groups at different conversion values. The figure clearly evidences the furan peak decreasing as conversion becomes in favour of benzyl-OH groups (*i.e.* out-of-plane C–H bending). All prepared polymers were characterized, before cross-linking, by DSC analysis (Fig. 5).

Polymers with only one functional group (either Fu or OH) display a monotonous increase of  $T_g$  with the amine conversion (Fig. 5A). This is in agreement with the increased rigidity of the backbone by increasing the amount of pyrrole groups.

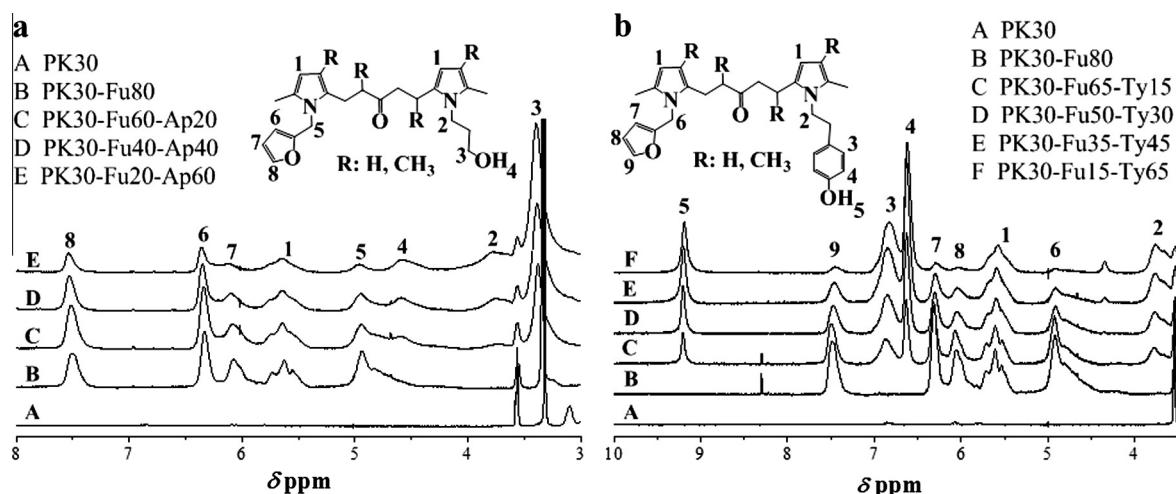


**Fig. 3.**  $^1\text{H}$  NMR spectra of PK30 modified with different ratios between furane (Fu) and OH groups (aliphatic-OH (a) and aromatic-OH (b)) at a maximal 80% of conversion.

Moreover, PK30 functionalized with aromatic OH groups (PK30-Ty) systematically displays (at equal conversion values) significantly higher  $T_g$  than those modified with furane (PK30-Fu) and aliphatic OH groups (PK30-Ap). This behaviour can be attributed to both the bulkiness of aromatic groups compared to aliphatic ones (compare PK30Ba80 with PK30Bea80 in Fig. 5B) which increases the steric hindrance so that the energy demand to activate segmental motions, and the relevant contribution (differences are up to 60 °C) provided by hydrogen bonding interactions (compare PK30Ap80 with PK30Ba80 and PK30Ty80 with PK30Bea80 respectively, Fig. 5B). The higher  $T_g$  value displayed by PK30-Ty compared to PK30-Ap can also be possibly due to the more acidic nature of phenyl-OH groups. This feature can be confirmed by the broad character of signals associated to hydrogen bonding of OH groups around  $3420\text{--}3390\text{ cm}^{-1}$  and considering the evident bathochromic shift ( $30\text{ cm}^{-1}$  for PK30-Fu-Ty) by increasing the amount of tyramine moieties (Fig. 4B). As expected, samples of the PK30-Fu-OH series (thus displaying the presence of both hydrogen bonding and possibly aromatic interactions (e.g. PK30-Fu-Ty)) show  $T_g$  values intermediate between the ones of the two reference compounds (PK30-Fu80 and PK30-OH80) at the same total conversion value (Fig. 5C). It is interesting to note in Fig. 5C a deviation from linearity for PK30-Fu65-Ty15. This can possibly be ascribed to the total lower conversion of this system, compared to the others (see Table 1).<sup>1</sup> It is worth noting that all DSC data clearly demonstrate, even before cross-linking, the remarkable versatility of the employed synthetic approach in yielding polymeric systems with tuneable thermal behaviour as a function of composition.

On the other hand, it can also be speculated that  $T_g$  values may come from undesired cross-linking reactions occurring during the polymer modifications. In order to clarify this point, Gel Permeation Chromatography analysis was performed on the different products (SI1). According to these results, it can be recognized that all systems display similar values of the polydispersity index (PDI) and practically the same magnitude of  $M_n$  and  $M_w$ , which proves that the different values obtained for  $T_g$  are only consequences of pyrrole formation, inter-polymeric interactions of functional groups and steric hindrance according to the bulkiness of each modifier as above mentioned.

The polymers were then cross-linked and de-cross-linked via a DA and r-DA sequence using an aromatic bis-maleimide (Fig. 6).

The cross-linking reactions of PK30-Fu and PK30-Fu-OH with bis-maleimide occurred at 50 °C for 24 h. All prepared samples were cross-linked with bis-maleimide in a ratio 1:1 between furane and maleimide groups. In a first step, DSC analysis was carried out in order to investigate the thermal behaviour of the prepared samples (Fig. 7).

In the heating and cooling runs, the occurrence of the Diels-Alder reaction (exothermic peaks) and its reverse process (endothermic peaks) are clearly visible. It is worth noting that each sample showed practically the same thermogram curves up to 3 cycles between 0 and 180 °C, thus confirming the full system reversibility. Moreover, the endothermic transition phase in all samples took place over a broad range of temperatures that reached values up to twenty degrees from the beginning to the end of the r-DA (i.e. the highest peak in the endothermic transition phase).

On the other hand, it is worth mentioning that the r-DA enthalpy (i.e. the area under the curve associated to the r-DA peak) is related to the energy required to break all DA adducts in each particular cross-linked system. According to this, one could assume in advance that the system containing the higher amount of furan/maleimide adducts (e.g. PK30-Fu80/Ma) should display the higher value of enthalpy when compared to those samples displaying the combination with Fu/b-Ma and

<sup>1</sup> We are grateful to the anonymous reviewer #1 for this observation.

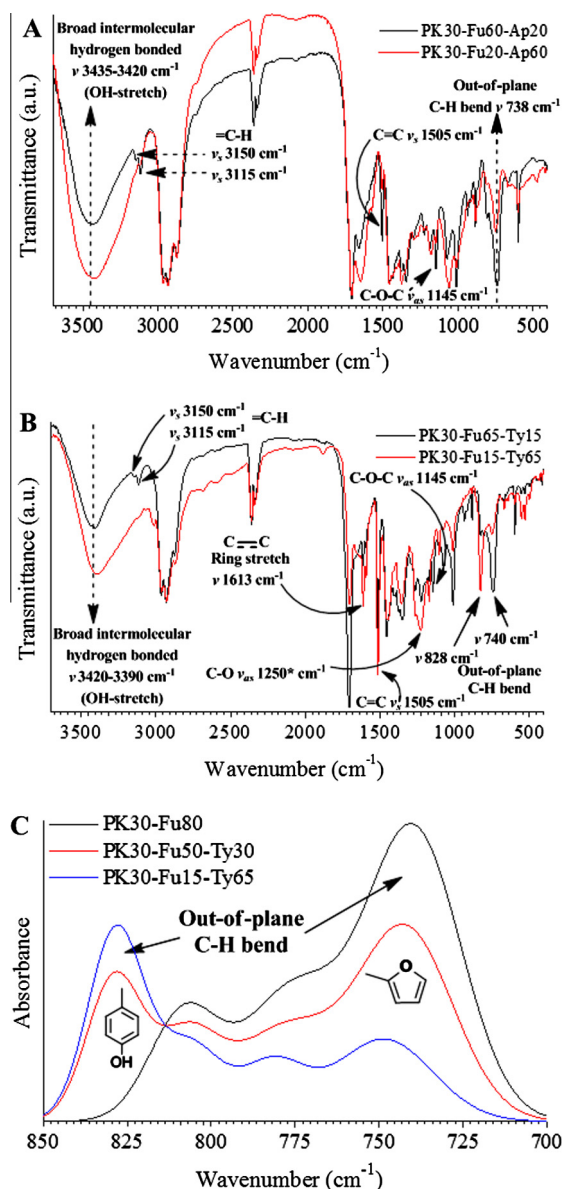


**Fig. 4.** FT-IR spectra of PK30 functionalized with furan/OH groups at different ratios, aliphatic OH (A) and aromatic OH (B). Figure (C) displays the magnification in the C–H bending region for (B) (furan peak 742  $\text{cm}^{-1}$  and benzene peak 827  $\text{cm}^{-1}$ ). Bands normalized at 2962  $\text{cm}^{-1}$  (C–H stretch).

hydrogen bonding OH groups. Indeed, the enthalpy value decreases (Fig. 7A = 33.66 J/g > 7B = 11.18 J/g > 7C = 8.17 J/g) with decreasing amount of DA adducts. Notably, the almost quantitative overlap of the endothermic and exothermic traces clearly indicates the reversibility of the systems upon thermal treatment at least in terms of amount of DA adducts broken and formed, respectively.

The thermo-mechanical behaviour of all prepared samples (as solid bars) was tested by DMTA at four heating cycles. DMTA results demonstrated that the corresponding softening point (taken as peak of  $\tan(\delta)$  in the corresponding DMTA curves) increases with the amount of furan/maleimide adducts in systems bearing only Fu groups. This is expected on the basis of the corresponding network density (Fig. 8).

In systems containing both Fu and OH functional groups (*i.e.* same 80% of carbonyl conversion along the backbone), the corresponding softening point decreases with the relative amount of OH groups (*i.e.* hydrogen bonding interactions) with respect to the furan ones (*i.e.* DA adduct). The trend is not linear with composition (or at least it does not seem to follow a linear pattern) since hydrogen bonding between OH groups and the carbonyl ones on the bis-maleimide compound might also take place and thus decrease the amount of available OH groups. In addition, the recovery of mechanical properties (modulus in this case) seems to be fully quantitative for both PK30-Fu (Fig. 9A) and PK30-Fu-OH (Fig. 9B and C; for brevity only three samples are shown).



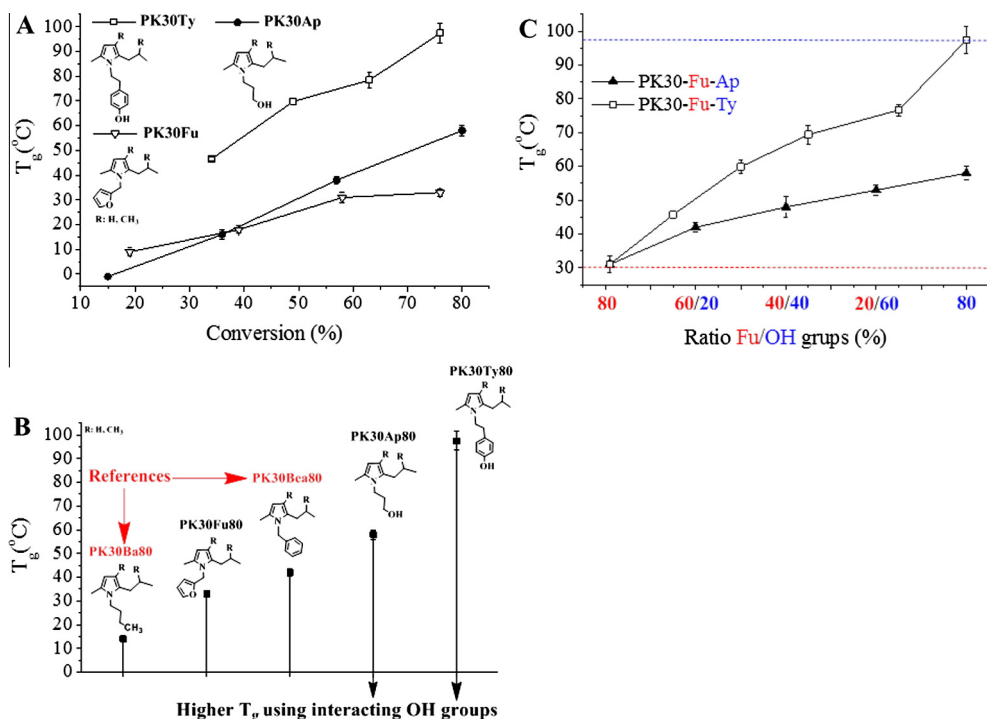


**Fig. 5.**  $T_g$  (measured by DSC) of PK30: as a function of different percentage of conversion with furfurylamine (PK30Fu), 3-amino-1-propanol (PK30Ap) and tyramine (PK30Ty) (A), as a function of different interacting side groups but same (~80%) total conversion and backbone structure (B) and as a function of different Fu/OH ratios at 80% total conversion (C).

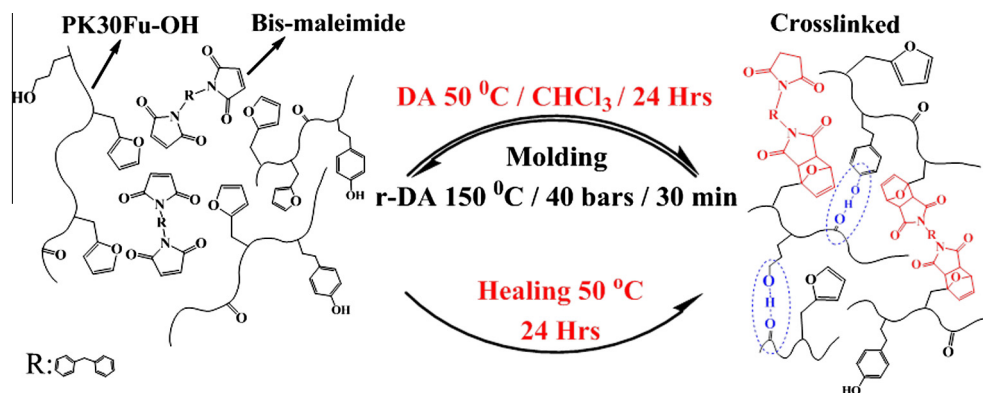


**Fig. 6.** Schematic representation of DA/r-DA sequence and molding of functionalized polyketone PK-Fu-OH cross-linked with bis-maleimide. In red reversible covalent interactions and blue hydrogen bonding (aliphatic or aromatic). (For interpretation of the references to color in this figure legend, the reader is referred to the web version of this article.)

Despite the relatively high softening point and the fully quantitative recovery of modulus during the thermal cycles and recycling (grained samples), the formation of reversible cross-linking through DA adducts seems to be a better option for the creation of materials with higher damping capabilities. However, the combination with hydrogen bonding discloses very interesting and promising pathways towards the design of tuneable (in terms of thermal properties) reversible thermosets. Actually, considerable compensation of the lower cross-linking density (due to the reduced amount of furan moieties) by hydrogen bonding is observed. In fact, by comparing the three different systems in Fig. 9, it is possible to see that the elastic and loss modulus are increased by the contribution of hydrogen bonding. It is worth mentioning that the ratio  $E''/E' = \tan \delta$  (right axes in Fig. 9) reach values of  $9A = 0.15 < 9C = 0.28 < 9B = 0.32$  indicating the formation of more elastic materials by decreasing the Diels-Alder crosslink density, respectively.

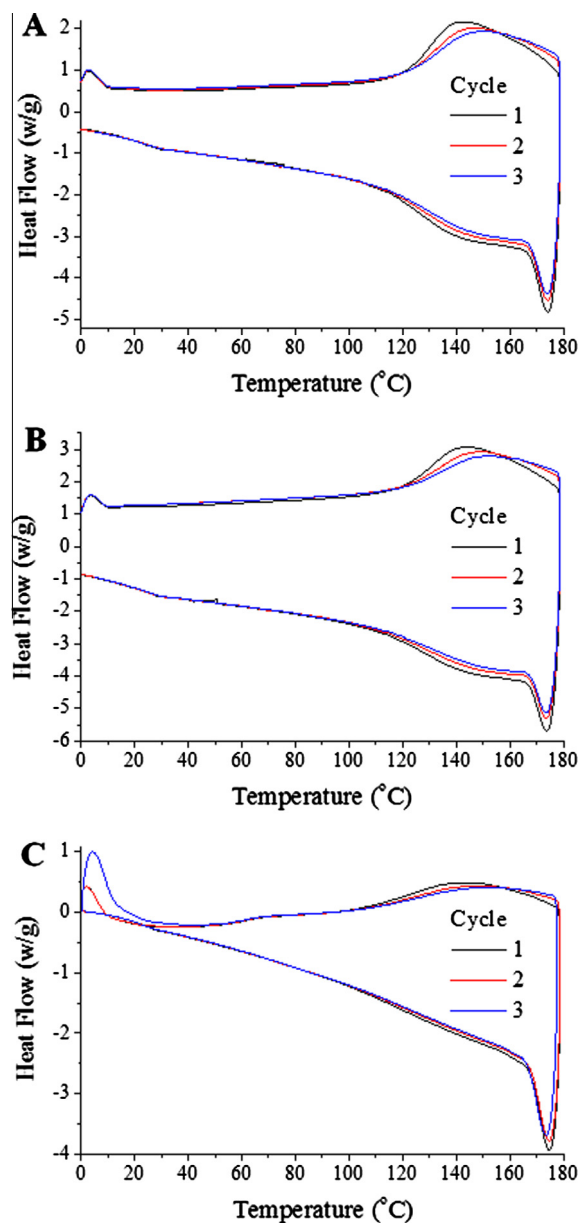


**Fig. 7.** DSC thermal cycles of cross-linked PK30-Fu80 (A), PK30-Fu40-Ap40 (B), PK30-Fu35-Ty45 (C). Ratio Fu/Maleimide = 1. Only three samples are showed for brevity.

In these particular systems (PK-Fu-OH), the addition of OH groups is crucially from two different points of view:

- from a scientific perspective it allows comparing polymers with the same backbone structure (*vide supra*), which in turn allows pinpointing the exact influence of hydrogen bonding on the thermal and mechanical behaviour;
- from an applicative point of view, it provides an easy and straightforward way to modulate the softening point of the final product while decreasing the chance of side reactions due to the fact that the carbonyl conversion is factually close to its theoretical maximum of 80% [37]. Moreover, the presence of OH groups increases the internal motion (friction) and relaxation of the polymeric chains during the applied stress. This certainly increases the intrinsic self-healing properties of the materials. It can be noticed by the fact that elastic and loss modulus remains practically as the original in continuous DMTA measurements (Fig. 9) due to the faster recovery of the hydrogen bonds.

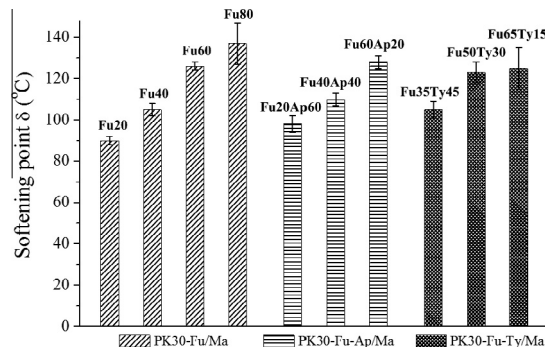


**Fig. 8.** Softening points ( $\tan \delta$ ) tested by DMTA of PK30-Fu at different grade of conversions and PK30-Fu-OH systems at different ratios of functional groups cross-linked with bis-maleimide. Ratio Fu/Maleimide 1:1.

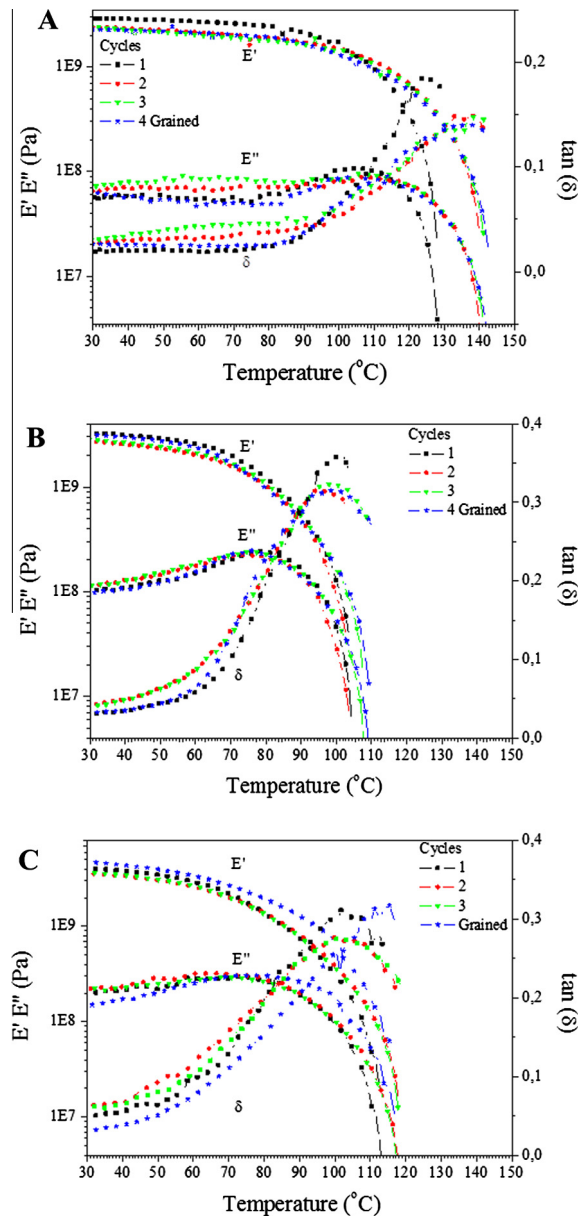


**Fig. 9.** Dynamic thermo-mechanical behaviour of cross-linked PK30-Fu80 (A). PK30-Fu20-Ap60 (B). PK30-Fu35-Ty45 (C). E': storage modulus, E'': loss modulus and Tan  $\delta$ : softening point (dumping factor). Ratio Fu/Maleimide = 1.

#### 4. Conclusion

This work illustrates the facile synthesis of intrinsic thermally self-healing polymeric material based on the chemical modification of aliphatic polyketones by Paal-Knorr reaction. The modification of the polymers was proved to be feasible using conventional oil bath and microwaves pathways to achieve similar end-products. Besides the easiness of the modification procedure, which constitutes a relevant novelty in the open literature, the Paal–Knorr reaction with aliphatic and aromatic amine compounds provides a series of general advantages. In particular it allows the preparation of a series of compounds displaying the exact backbone structure but a (systematic) variation in the amount of hydrogen bonding and Diels–Alder active groups. From a scientific perspective this allows to pinpoint exactly the influence of both kinds of interactions on the thermal and mechanical behaviour. Indeed, DSC traces indicated that furan/OH-functionalized polyketones are capable to be repeatedly cross-linked and de-cross-linked with bis-maleimide by only using heat as external stimulus. Furthermore, DMTA measurements testify the relevant contribution of Diels–Alder covalent bonding to the final softening point temperature while hydrogen bonding interactions seem to contribute with faster quantitative recovery of modulus in these systems.

#### Appendix A. Supplementary material

Supplementary data associated with this article can be found, in the online version, at <http://dx.doi.org/10.1016/j.eurpolymj.2016.06.004>.

#### References

- [1] S. Rajendran, A. Hodzic, C. Soutis, M.A. Al-Maadeed, Review of life cycle assessment on polyolefins and related materials, *Plast. Rubber Compos.* 41 (4–5) (2012) 159–168.
- [2] H. Nishida, Development of materials and technologies for control of polymer recycling, *Polym. J.* 43 (5) (2011) 435–447.
- [3] J. Henshaw, W. Han, A. Owens, An overview of recycling issues for composite materials, *J. Thermoplast. Compos. Mater.* 9 (1) (1996) 4–20.
- [4] Y. Yang, R. Boom, B. Irion, D. van Heerden, P. Kuiper, H. de Wit, Recycling of composite materials, *Chem. Eng. Process.* 51 (2012) 53–68.
- [5] S. Pimenta, S.T. Pinho, Recycling carbon fibre reinforced polymers for structural applications: technology review and market outlook, *Waste Manage.* 31 (2) (2011) 378–392.
- [6] S. Pickering, Recycling technologies for thermoset composite materials – current status, *Compos. Part A – Appl. Sci. Manuf.* 37 (8) (2006) 1206–1215.
- [7] European Commission, Report from the Commission to the European Parliament, the Council, the European Economic and Social Committee and the Committee of the Regions, on the Thematic Strategy on the Prevention and Recycling of Waste 2011, COM 13 Final (SEC 70 Final).
- [8] V. Goodship, Introduction to Plastics Recycling, Smithers Rapra Technology Limited, Shrewsbury, UK, 2007.
- [9] V. Andreoni, H.G.M. Saveyn, P. Eder, Polyethylene recycling: waste policy scenario analysis for the EU-27, *J. Environ. Manage.* 158 (2015) 103–110.
- [10] H.J. Koo, G.S. Chang, S.H. Kim, W.G. Hahm, S.Y. Park, Effects of recycling processes on physical, mechanical and degradation properties of PET yarns, *Fibers Polym.* 14 (12) (2013) 2083–2087.
- [11] M.Q. Zhang, M.Z. Rong, Intrinsic self-healing of covalent polymers through bond reconnection towards strength restoration, *Polym. Chem.* 4 (18) (2013) 4878–4884.
- [12] S.H. Cho, H.M. Andersson, S.R. White, N.R. Sottos, P.V. Braun, Polydimethylsiloxane-based self-healing materials, *Adv. Mater.* 18 (8) (2006) 997–1000.
- [13] X. Liu, J.K. Lee, S.H. Yoon, M.R. Kessler, Characterization of diene monomers as healing agents for autonomic damage repair, *J. Appl. Polym. Sci.* 101 (3) (2006) 1266–1272.
- [14] J.W.C. Pang, I.P. Bond, A hollow fibre reinforced polymer composite encompassing self-healing and enhanced damage visibility, *Compos. Sci. Technol.* 65 (11–12) (2005) 1791–1799.
- [15] J.W.C. Pang, I.P. Bond, 'Bleeding composites' – damage detection and self-repair using a biomimetic approach, *Compos. Part A – Appl. Sci. Manuf.* 36 (2) (2005) 183–188.
- [16] S. White, N. Sottos, P. Geubelle, J. Moore, M. Kessler, S. Sriram, E. Brown, S. Viswanathan, Autonomic healing of polymer composites, *Nature* 409 (6822) (2001) 794–797.
- [17] K.N. Long, The mechanics of network polymers with thermally reversible linkages, *J. Mech. Phys. Solids* 63 (2014) 386–411.
- [18] C. Nielsen, H. Weizman, S. Nemat-Nasser, Thermally reversible cross-links in a healable polymer: estimating the quantity, rate of formation, and effect on viscosity, *Polymer* 55 (2) (2014) 632–641.
- [19] R. Zhang, S. Yu, S. Chen, Q. Wu, T. Chen, P. Sun, B. Li, D. Ding, Reversible cross-linking, microdomain structure, and heterogeneous dynamics in thermally reversible cross-linked polyurethane as revealed by solid-state NMR, *J. Phys. Chem. B* 118 (4) (2014) 1126–1137.
- [20] R. Araya-Hermosilla, A.A. Broekhuis, F. Picchioni, Reversible polymer networks containing covalent and hydrogen bonding interactions, *Eur. Polym. J.* 50 (2014) 127–134.
- [21] Y. Song, C. Chung, Repeatable self-healing of a microcapsule-type protective coating, *Polym. Chem.* 4 (18) (2013) 4940–4947.
- [22] Z. Wang, M.W. Urban, Facile UV-healable polyethylenimine-copper (C<sub>2</sub>H<sub>5</sub>N-Cu) supramolecular polymer networks, *Polym. Chem.* 4 (18) (2013) 4897–4901.
- [23] J.M. Chang, J.J. Aklonis, A photothermal reversibly crosslinkable polymer system, *J. Polym. Sci. Part C – Polym. Lett.* 21 (12) (1983) 999–1004.
- [24] Q. Zhang, D. Qu, J. Wu, X. Ma, Q. Wang, H. Tian, A dual-modality photoswitchable supramolecular polymer, *Langmuir* 29 (17) (2013) 5345–5350.
- [25] M. Burnworth, L. Tang, J.R. Kumpfer, A.J. Duncan, F.L. Beyer, G.L. Fiore, S.J. Rowan, C. Weder, Optically healable supramolecular polymers, *Nature* 472 (7343) (2011) 334–338.
- [26] K. Ishida, V. Weibel, N. Yoshie, Substituent effect on structure and physical properties of semicrystalline Diels–Alder network polymers, *Polymer* 52 (13) (2011) 2877–2882.
- [27] D. Döhler, P. Michael, W. Binder, in: W.H. Binder (Ed.), *Principles of Self-Healing Polymers*, Wiley-VCH Verlag GmbH and Co., Weinheim, Germany, 2013, p. 66.
- [28] W.G. Skene, J.-M. Lehn, Dynamers: polyacylhydrazone reversible covalent polymers, component exchange, and constitutional diversity, *Proc. Natl. Acad. Sci. USA* 101 (22) (2004) 8270–8275.
- [29] S.P. Khor, R.J. Varley, S.Z. Shen, Q. Yuan, Thermo-reversible healing in a crosslinked polymer network containing covalent and thermo-reversible bonds, *J. Appl. Polym. Sci.* 128 (6) (2013) 3743–3750.
- [30] T. Ware, K. Hearon, A. Lonnecker, K.L. Wooley, D.J. Maitland, W. Voit, Triple-shape memory polymers based on self-complementary hydrogen bonding, *Macromolecules* 45 (2) (2012) 1062–1069.
- [31] Y. Chen, Z. Guan, Self-assembly of core-shell nanoparticles for self-healing materials, *Polym. Chem.* 4 (18) (2013) 4885–4889.

- [32] Y. Zhang, A.A. Broekhuis, F. Picchioni, Thermally self-healing polymeric materials: the next step to recycling thermoset polymers?, *Macromolecules* 42 (2009) 1906–1912
- [33] E. Drent, J. Keijsper, *Polyketone Polymer Preparation with Tetra Alkyl Bis Phosphine Ligand and Hydrogen*, 1993, US 5225523.
- [34] W.P. Mul, H. Dirkzwager, A.A. Broekhuis, H.J. Heeres, A.J. van der Linden, A.G. Orpen, Highly active, recyclable catalyst for the manufacture of viscous, low molecular weight, CO-ethene-propene-based polyketone, base component for a new class of resins, *Inorg. Chim. Acta* 327 (2002) 147–159.
- [35] Y. Zhang, A.A. Broekhuis, F. Picchioni, Thermally self-healing polymeric materials: the next step to recycling thermoset polymers?, *Macromolecules* 42 (6) (2009) 1906–1912
- [36] A.I.M. Hamarneh, *Novel Wood Adhesives from Bio-based Materials and Polyketones*, 2010.
- [37] C. Toncelli, D.C. De Reus, F. Picchioni, A.A. Broekhuis, Properties of reversible Diels–Alder Furan/maleimide polymer networks as function of crosslink density, *Macromol. Chem. Phys.* 213 (2) (2012) 157–165.
- [38] Y. Zhang, A.A. Broekhuis, M.C.A. Stuart, F. Picchioni, Polymeric Amines by chemical modifications of alternating aliphatic polyketones, *J. Appl. Polym. Sci.* 107 (1) (2008) 262–271.
- [39] A.I.M. Hamarneh, *Novel Wood Adhesives from Bio-based Materials and Polyketones*, 2010. 2:22.